Am J Transl Res 2026;18(2):932-948
www.ajtr.org /ISSN:1943-8141/AJTR0169209

*Original Article*

# Long non-coding RNA ZBTB46-AS1 promotes ovarian cancer progression through regulation of p53 activity by TAF6 protein

Liyu Wang[1,2*], Baoquan Liang[3*], Anquan Huang[2*], Luyao Zhang[2], Ying Feng[2], Guoqiang Wang[2], Fen Guo[2], Hong Xu[1]

[1]*Department of Oncology, The First Affiliated Hospital of Soochow University, Suzhou 215006, Jiangsu, China;* [2]*Department of Oncology, The Affiliated Suzhou Hospital of Nanjing Medical University, Suzhou Municipal Hospital, Gusu School, Nanjing Medical University, Suzhou 215008, Jiangsu, China;* [3]*Department of Gynecology, The Affiliated Suzhou Hospital of Nanjing Medical University, Suzhou Municipal Hospital, Gusu School, Nanjing Medical University, Suzhou 215008, Jiangsu, China.* [*]*Equal contributors.*

Received October 9, 2025; Accepted January 4, 2026; Epub February 15, 2026; Published February 28, 2026

**Abstract:** Objective: To elucidate the oncogenic role and molecular pathways associated with long non-coding RNA ZBTB46-AS1 (lncRNA ZBTB46-AS1) in ovarian cancer (OC) progression. Methods: Bioinformatics analyses of the Gene Expression Omnibus (GEO) and The Cancer Genome Atlas (TCGA) databases were used to assess ZBTB46-AS1 expression and prognostic value. Quantitative real-time polymerase chain reaction (qRT-PCR) verified its expression in 22 pairs of OC and adjacent normal tissues, as well as OC cell lines. In vitro functional assays [Cell Counting Kit-8 (CCK8), colony formation, Transwell] and in vivo models [xenograft, lung metastasis] were performed to evaluate the effects of ZBTB46-AS1 knockdown. RNA pull-down, RNA immunoprecipitation (RIP), dual-luciferase reporter, and co-immunoprecipitation (Co-IP) assays clarified its interaction with TATA-box-binding protein-associated factor 6 (TAF6) and tumor suppressor protein p53. Results: ZBTB46-AS1 was significantly upregulated in OC tissues and cell lines, correlating with poor overall survival (OS) of patients. Stable knockdown of ZBTB46-AS1 inhibited the proliferation, colony formation, and epithelial-mesenchymal transition (EMT) of OC cells in vitro, as well as tumor growth and distant metastasis in vivo. Mechanistically, ZBTB46-AS1 directly interacted with TAF6, which attenuated the binding between TAF6 and p53, suppressed p53 transcriptional activity, and consequently downregulated the expression of p21. Notably, co-silencing of ZBTB46-AS1 and p53 effectively reversed the inhibitory effects induced by ZBTB46-AS1 knockdown on OC cell malignant phenotypes. Conclusion: ZBTB46-AS1 promotes OC progression via the TAF6-p53 axis, serving as a potential prognostic marker and therapeutic target.

**Keywords:** Ovarian cancer, lncRNA ZBTB46-AS1, TAF6, p53, tumorigenesis

## Introduction

Ovarian cancer (OC) ranks as one of the most frequently occurring and fatal gynecological cancers. In 2023, the United States recorded 19,710 new ovarian cancer cases and 13,270 deaths as reported by the American Cancer Society annual statistical analysis. OC is the fifth most common cause of cancer-related death in women, followed by lung, breast, colorectal, and pancreatic cancers, accounting for 5% of all cancer-related mortalities [1]. Patients with advanced-stage OC have limited treatment options, resulting in a poor prognosis and high mortality rates [2]. The unique genetic and phenotypic traits of ovarian carcinoma contribute to tumor promotion and development of chemoresistance and disease recurrence. Furthermore, the ability of OC to undergo epithelial-mesenchymal transition (EMT), which is strongly linked to tumor growth and metastasis, presents a significant barrier for effective treatment. Therefore, the discovery of novel therapeutic targets has become increasingly important.

Contemporary genomic analyses employing high-density oligonucleotide arrays and mas-

https://doi.org/10.62347/LTBC2414

sively parallel sequencing platforms have unequivocally demonstrated that protein-coding regions span merely 1.2-2.3% of the human genome, while the non-coding majority generates a complex repertoire of functionally active transcripts [3, 4]. A burgeoning body of studies indicate that ncRNAs play crucial regulatory roles in complex growth and developmental processes [5, 6]. In particular, long non-coding RNAs (lncRNAs), which range in length from 200 to 100,000 nucleotides, constitute a significant proportion of all non-coding RNAs (ncRNAs). They interact with proteins, DNA, and other RNA molecules through diverse mechanisms to modulate gene expression across various levels, including epigenetic, transcriptional, and post-transcriptional regulation [7, 8].

Advancements in biomedicine have facilitated the identification and functional characterization of lncRNAs. Recent investigations have demonstrated that the dysregulation of various lncRNAs is a common feature in human diseases, with a significant impact on the initiation and development of tumors. Aberrantly expressed lncRNAs can alter cellular biological processes and act as significant mediators of tumor malignancy [9]. In this study, through a literature review and in-depth analysis of OC databases, we identified ZBTB46-AS1 as a newly discovered lncRNA that plays a significant role in the initiation and development of OC. The upregulation of ZBTB46-AS1 was significantly correlated with poor prognosis in patients with OC, as validated in the clinical samples collected in our study.

ZBTB46, alternatively designated BTBD4, zDC, or BZEL, is a member of the POZ and BTB (ZBTB) protein family [10]. Prior research has demonstrated that ZBTB46 acts as a transcription factor that is specifically expressed in classical dendritic cells (cDCs), with selective expression in pre-DCs and cDCs, and is instrumental in maintaining these cells in a quiescent state [11]. Recent research has proposed that ZBTB46 is a shared transcription factor between cDCs and group 3 innate lymphoid cells (ILC3s), and has been identified to have an intrinsic cellular function in inhibiting the pro-inflammatory characteristics of ILC3s that play a role in the coordination of intestinal health [12]. ZBTB46-AS1, an antisense long non-coding RNA situated on the antisense strand of the ZBTB46 gene, may regulate the expression levels of ZBTB46 and thereby affect cellular biological functions. To date, there have been no studies on ZBTB46-AS1 and its specific mechanism of action in OC remains unclear. In this study, we conducted a comprehensive analysis of the expression and prognostic implications of ZBTB46-AS1 in OC, with the aim of identifying novel targets and biomarkers that could enhance the diagnosis, treatment, and prognosis of this disease.

## Materials and methods

### *Bioinformatics analysis*

The gene chip datasets GSE18520 and GSE74448 were obtained from the Gene Expression Omnibus (GEO) database. The GSE18520 dataset contains transcriptome microarray data from 10 normal ovarian epithelial tissues and 53 ovarian cancer samples. Transcriptome microarray data from 11 normal ovarian epithelial tissue samples and 29 ovarian cancer samples were included in the GSE74448 dataset. The TCGA database was utilized to construct Kaplan-Meier survival curves, thereby examining the association between ZBTB46-AS1 expression and the prognosis of patients with OC.

### *Patient samples collection*

Samples from patients with primary OC who underwent surgical treatment were collected between October 2020 and December 2022 at the Department of Obstetrics and Gynecology of Suzhou Municipal Hospital, affiliated with Nanjing Medical University. Normal tissue samples were obtained from the paired adjacent tissues. None of the patients received radiotherapy or chemotherapy before undergoing surgical intervention. Appropriate tissue samples were excised during surgery and immediately placed in prepared cryovials, which were then temporarily stored in liquid nitrogen tanks before being transferred to a -80°C freezer for extended safekeeping. For this study, 22 ovarian cancer tissue specimens were collected together with their corresponding clinical data. Before sample collection, informed consent was obtained from all participants, and the research protocol was approved by the Ethics Committee of Suzhou Municipal Hospital, affili-

ated with Nanjing Medical University (approval number: K-2025-002-K02).

*Cell line and cell culture*

This study employed the following human OC cell lines: SKOV3, A2780, OVCAR3, and H08910. The normal control cell line was IOSE80, which is an ovarian epithelial cell line. The cell lines were obtained from Zhongqiaoxinzhou Biotech (Shanghai, China). IOSE80 cells were cultured in DMEM, while SKOV3 and A2780 cells were maintained in RPMI-1640 medium (Invitrogen, Carlsbad, CA, USA) supplemented with 10% fetal bovine serum (FBS). Cells were incubated at 37°C in a humidified environment containing 5% $CO_2$ and 95% air.

*Cell transfection*

Small interfering RNA (siRNA) sequences, sh-lncRNA ZBTB46-AS1, overexpression control plasmids(vector), and TAF6 overexpression plasmids were synthesized by GenePharma (Shanghai, China). Following a 48-hour transfection period utilizing Lipofectamine 2000 (Invitrogen, CA, USA), cells were collected for further experiments. RT-qPCR was conducted to analyze the cell transfection efficiency. The specific siRNA sequences used in this study are as follows: si-ZBTB46-AS1 1#, 5-GGGACUACAGAAACAUGAA-3; si-ZBTB46-AS1 2#, 5'-GCUGGGAGAACCGGGAAUA-3'; si-NC, 5'-UUCUCCGAACGUGUCACGU-3'.

*qRT-PCR RNA extraction and qRT-PCR assays*

Total RNA was isolated from cells using TRIzol reagent (Vazyme, Nanjing, China) in accordance with the manufacturer's protocol. The extracted RNA was converted into complementary DNA (cDNA) through the use of a reverse transcription kit (Vazyme, Nanjing, China). cDNA templates were subjected to qPCR amplification using SYBR qPCR SuperMix Plus (Novoprotein Scientific Inc., Shanghai, China) and an Applied Biosystems 7500 Fast Real-Time PCR system [13, 14]. The primers used in the experiments were as follows: ZBTB-AS1-F, TCAAGCGGAACCGATACACT; ZBTB-AS1-R, TTATTCCCGGTTCTCCCAGC; 18sRNA-F, AAACGGCTACCACATCCAAG; 18sRNA-R, CCTCCAATGGATCCTCGTTA; p21-F, GGCAGACCAGCATGACAGATTT; p21-R, AGATGTAGAGCGGGCCTTTG.

*Cell Counting Kit 8 (CCK8) assay*

A2780 and SKOV3 cells in the logarithmic growth phase were selected. The cells were resuspended in the culture medium and their concentration was adjusted to $1.5\times10^4$ cells/mL. The cells were dispensed into a 96-well cell culture plate, with each well filled with 200 μL of cell suspension. Cell proliferation was assessed at five time points (0, 24, 48, 72, and 96 h). The plates were gently mixed and incubated at 37°C. The 96-well plate was removed at the indicated time points and 20 μL of CCK-8 solution (Beyotime Biotechnology, Nantong, China) was added to each well. The plates were incubated for four hours at 37°C in the dark. Cell viability was assessed by measuring the optical density at 450 nm (OD450) using a microplate reader (Bio-Rad Model 680; Richmond, CA, USA) and plotting the growth curves. Each experiment was performed in triplicate.

*Cell clonal formation experiment*

The cells were placed in a six-well plate and cultured for 14 days. During this period, the culture medium was renewed every three days and subsequently discarded. The cells were fixed with methanol for 30 min, stained with 0.1% crystal violet (Beyotime Biotechnology) for 30 min, and subsequently dried. Visible colonies were then identified and counted. The experiment was repeated three times.

*Cell migration assays*

Transwell chambers (8 μm aperture; Millipore, Billerica, MA, USA) were placed in a 24-well plate. A2780 and SKOV3 cell suspensions in a logarithmic growth stage were inoculated into the upper chamber at a density of $1.5\times10^5$ cells/mL, and 700 μL medium containing 10% Fetal Bovine Serum (FBS) was added into the lower chamber and placed in an incubator containing 5% $CO_2$. The cells were cultured at 37°C for 48 h. Once completed, a moist cotton swab was used to wipe off the cells on the upper chamber and the membrane surface. The cells that migrated to the underside of the membrane were fixed with methanol for 15 min, stained with 0.1% crystal violet for 15 min, gently rinsed twice with PBS, and allowed to air dry at room temperature. Five fields were randomly selected for cell counting using a 100× invert-

ed microscope. The experiment was repeated three times.

*In vivo assays*

*Animals:* In this study, female BALB/c nude mice, aged four weeks and weighing approximately 20±2 grams, were utilized. The mice were obtained from the Nanjing Medical University Animal Facility and were housed under conditions that met specific pathogen-free criteria. The Animal Ethics Committee at Nanjing Medical University granted approval for the animal experiments. (approval number: 2004020).

*Xenograft tumor in nude mice:* Sh-ZBTB46-AS1 and an empty vector were stably transfected into the SKOV3 cells. Following transfection, the cells were collected and rinsed with PBS. The cells were resuspended in PBS at a concentration of $5\times10^7$ cells/ml. Subsequently, 100 μL of cells from the experimental and control groups were injected into the subcutaneous skin of each mouse beneath the armpit. In vivo cell proliferation assays were performed by examining and recording tumor growth every three days. After two weeks, the mice were euthanized by inhalation of $CO_2$ anesthesia following the American Veterinary Medical Association (AVMA) protocols for animal euthanasia (2020 edition). The mice were quickly rendered unconscious before being euthanized by cervical dislocation. Tumors were excised, weighed, and photographed. The calculation of tumor volume was performed using the following formula: Tumor volume ($mm^3$) = 0.5 × length (mm) × width$^2$ ($mm^2$), and a growth curve was plotted to record the tumor volume over time.

*Xenometastases in nude mice:* For the in vivo cellular metastasis assay, 100 μL of SKOV3 cells transfected with sh-ZBTB46-AS1 or sh-NC (suspended at a concentration of $6\times10^7$ cells/mL) were injected into the tail veins of mice. Mice in both groups were euthanized eight weeks after inoculation. The lung tissue samples were extracted, weighed, and photographed. The size and number of lung metastatic tumors were calculated, and lung metastatic sections were stained with hematoxylin and eosin (H&E) for pathological examination.

*Immunofluorescence*

The paraffin sections were deparaffinized with xylene and rehydrated in a series of decreasing concentrations of ethanol. Antigen retrieval was performed by incubating the sections for 20 minutes in sodium citrate buffer (pH 6.0). After washing with PBS, sections were incubated with primary antibodies overnight at 4°C. After another round of PBS washing, the sections were incubated with secondary antibodies for 1 h at room temperature. DAPI (Beyotime Biotechnology) staining was performed and the sections were incubated for 10 min at room temperature. Images were captured using a Zeiss LSM800 laser scanning microscope (Carl Zeiss, Oberkochen, Germany) [15]. The antibodies used were as follows: mouse monoclonal anti-Ki67 antibody (Abcam, ab238020, 1:100), mouse monoclonal anti-E-cadherin antibody (Abcam, ab231303, 1:100), mouse monoclonal anti-N-cadherin antibody (Abcam, ab76057, 1:100), and mouse monoclonal anti-Vimentin antibody (Abcam, ab20346, 1:100).

*RNA pull-down assays*

The Ribo RNAmax-T7 Biotin RNA Labeling Kit (RiboBio, Guangzhou, China) was used to perform the assay. T7 RNA polymerase (Ambion Life Technologies) was used to transcribe ZBTB46-AS1, which was purified using the RNeasy Plus Mini Kit (Qiagen) and treated with RNase-free DNase I (Qiagen). Next, the transcribed ZBTB46-AS1 was biotin-labeled using Biotin RNA Labeling Mix (Ambion Life Technologies), as directed by the manufacturer. The Pierce™ Magnetic RNA-Protein Pull-Down Kit (Thermo Fisher Scientific) was used to perform the RNA pull-down assay following the aforementioned experimental protocols [16]. The proteins interacting with ZBTB46-AS1 were identified by liquid chromatography-tandem mass spectrometry (LC-MS/MS) as previously described [17-20].

*RNA immunoprecipitation assays*

The RIP (RNA Immunoprecipitation) assay was conducted using the EZ-Magna RIP™ RNA-Binding Protein Immunoprecipitation Kit (Millipore, Billerica, MA, USA). Briefly, SKOV3 cells were cultured and lysed in a radioimmunoprecipitation (RIP) lysis buffer. A total of 100 μL of the cell lysate was incubated overnight at 4°C with magnetic beads conjugated to either anti-human TAF6 antibody or normal mouse IgG (negative control). The protein-RNA complexes were captured, and proteins were digested with proteinase K. The magnetic beads were washed

multiple times with the RIP wash buffer to eliminate nonspecific binding. Finally, purified RNA was subjected to RT-qPCR to assess TAF6 binding.

*Dual-luciferase reporter assay*

To assess the regulatory effects of ZBTB46-AS1 and TAF6 on p53 activity, we constructed a firefly luciferase reporter plasmid containing p53 response elements (pp53-TA-luc) and Renilla luciferase control plasmid (Beyotime, Shanghai). We established various transfection groups and used Lipofectamine 2000 to co-transfect these plasmids with siRNA targeting ZBTB46-AS1 and TAF6, or their respective overexpression plasmids, into A2780 and SKOV3 cells. After 48 h of incubation, luciferase activity was assessed using the Dual-Luciferase Reporter Assay Kit (Promega, Madison, WI, USA).

*Immunoprecipitation*

At this stage, the culture medium was removed and the cells were washed three times with PBS. The supernatant was discarded after the cells were digested and resuspended and IP lysis buffer (containing protease inhibitors) was added and incubated on ice for 30 min to facilitate cell lysis. The cell lysate was centrifuged at 12,000 rpm for 10 min at 4°C to obtain the supernatant. Protein A/G beads (20 μL) were added to the cell lysate and incubated with gentle shaking for two hours at 4°C to remove nonspecific binding. A magnetic rack was used to collect the supernatant and 5 μg of the corresponding antibody was added and incubated overnight at 4°C with gentle shaking. The following day, 50 μL of protein A/G beads were added to the antigen-antibody mixture and incubated for three hours at 4°C with gentle shaking. After collecting the supernatant using a magnetic rack, the protein A/G beads were washed thrice with lysis buffer. Finally, 40 μL of 1x loading buffer was added to the magnetic beads and boiled in a water bath for 10 min. The supernatant was discarded after centrifugation, and western blot analysis was performed.

*Statistical analysis*

GraphPad Prism 9.0 software (GraphPad Software, CA, USA) was used for data processing and statistical analysis. Numerical data are presented as mean ± standard deviation (SD). Chi-square analysis was used to assess categorical data. Concurrently, group differences were compared using the Wilcoxon rank-sum test, one-way analysis of variance (ANOVA), and two-tailed Student's t-test. Pearson or Spearman correlation coefficients were used to assess the correlations. The Kaplan-Meier technique was used to plot survival curves, and the log-rank test was used to analyze survival differences. Statistical significance was set at $P < 0.05$.

## Results

*The expression of ZBTB46-AS1 is upregulated in OC tissues and cell lines, indicating poor prognosis*

First, we used the Gene Expression Omnibus (GEO) database to perform differential gene expression analysis on the ovarian cancer-related expression datasets, GSE18520 and GSE74448. We identified a novel lncRNA linked to ovarian cancer, ZBTB46-AS1. Box plots demonstrated that ZBTB46-AS1 has a significantly higher expression in ovarian cancer tissues than in normal ovarian tissues (**Figure 1A** and **1B**). Patients with high ZBTB46-AS1 expression had substantially lower overall survival and disease-related survival rates than those with low expression (log-rank $P < 0.05$), according to Kaplan-Meier survival curves based on The Cancer Genome Atlas (TCGA) database (**Figure 1C** and **1D**). In addition, we used qRT-PCR to analyze the expression of ZBTB46-AS1 in 22 OC tumor tissues and matched neighboring non-tumor tissues. The findings revealed that ZBTB46-AS1 was upregulated in tumor specimens compared to that in adjacent non-tumor tissues (**Figure 1E**). We further examined the expression of ZBTB46-AS1 in SKOV3, A2780, H08910, and OVCAR3 cell lines using RT-qPCR, which showed higher expression levels of ZBTB46-AS1 in ovarian cancer cell lines than in the IOSE80 cell line, with SKOV3 and A2780 cells showing the highest expression levels (**Figure 1F**). The SKOV3 and A2780 cell lines were selected for further experiments.

*ZBTB46-AS1 promotes the proliferation and migration of OC in vitro*

To investigate the impact of ZBTB46-AS1 on OC cell proliferation and migration, we synthesized two ZBTB46-AS1 siRNAs (si-ZBTB46-AS1 1#

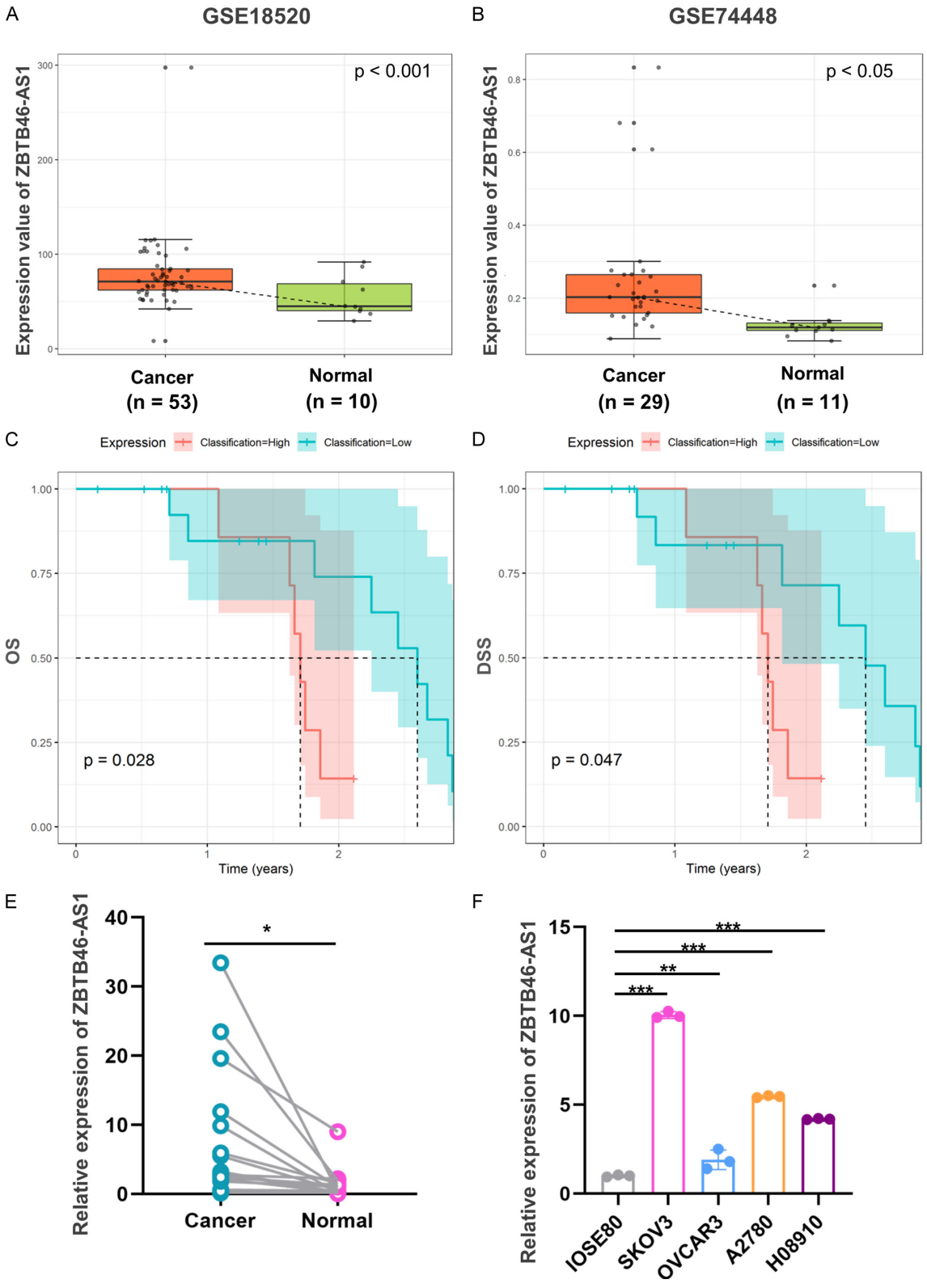


**Figure 1.** Analysis of ZBTB46-AS1 expression levels and its clinical implications in ovarian cancer (OC) tissues and cell lines. A, B. Relative expression of ZBTB46-AS1 based on GEO datasets. C, D. Kaplan-Meier curves of overall survival and disease-related survival in patients with OC based on TCGA data. E. Relative expression levels of ZBTB46-AS1 in OC tissues and paired adjacent non-cancerous tissues (n = 22). F. The expression of ZBTB46-AS1 in OC cell lines (SKOV3, OVCAR3, A2780, and H08910) and normal ovarian epithelial cells (IOSE80) were detected using RT-qPCR (n = 3). Statistical data are presented as mean ± SD. Significant differences were determined using Student's t-test. *P < 0.05, **P < 0.01 and ***P < 0.001.

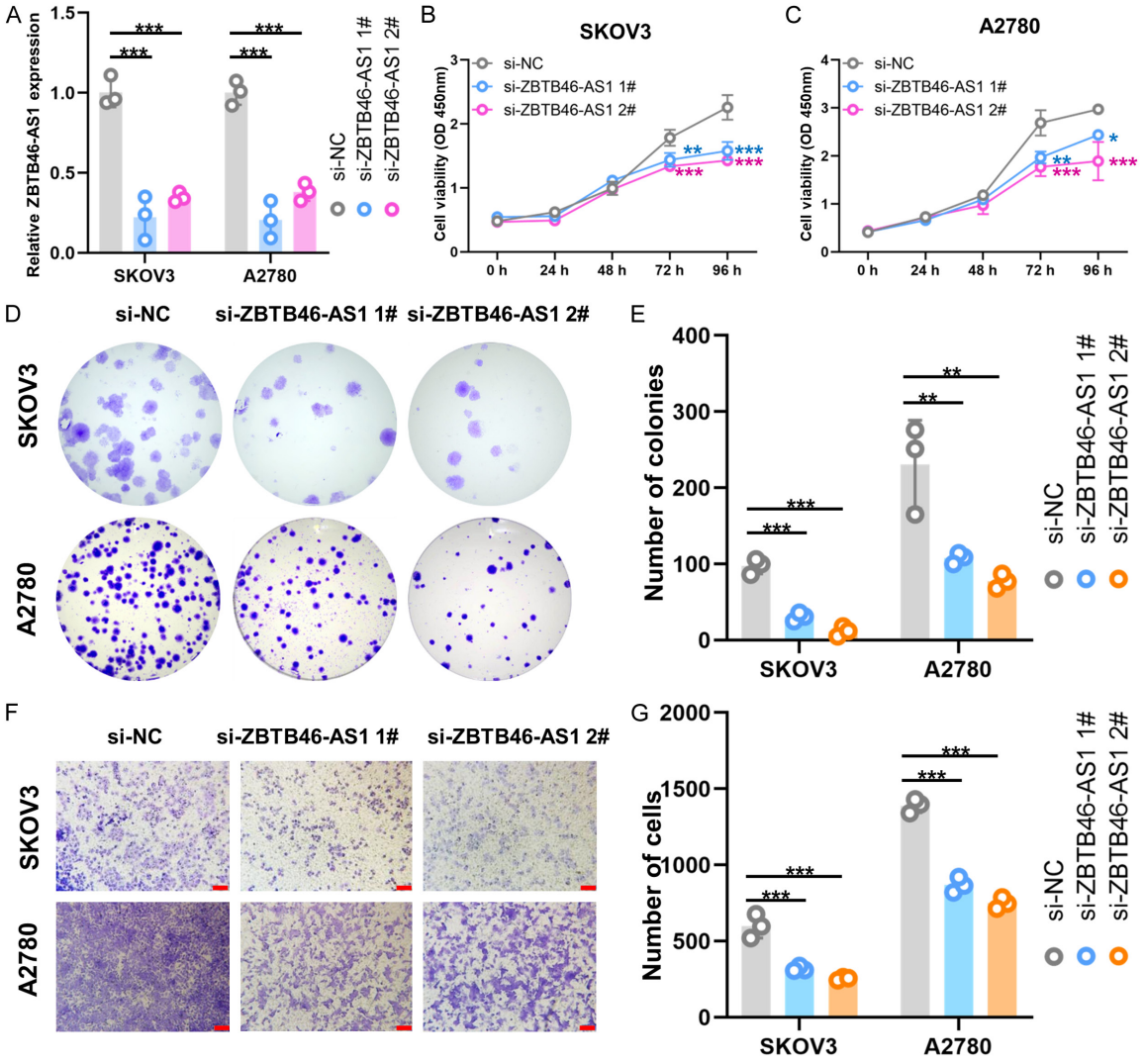


**Figure 2.** Effects of ZBTB46-AS1 knockdown on OC cell proliferation and migration in vitro. (A) ZBTB46-AS1 expression in SKOV3 and A2780 cells transfected with negative control siRNA (si-NC) or siRNAs targeting ZBTB46-AS1 (si-ZBTB46-AS1 #1 and #2) for 48 h (n = 3 for each group). (B, C) SKOV3 and A2780 cells were transfected with si-NC or si-ZBTB46-AS1, and cell viability was measured using CCK8 viability assay at specified time points (n = 3 per group). (D, E) Cell colony formation experiments were performed to determine the proliferative ability of si-ZBTB46-AS1 transfected (n = 3 for each group). (F, G) Transwell assays were conducted to evaluate the migratory capacity of SKOV3 and A2780 cells following the knockdown of ZBTB46-AS1 (n = 3). Scale bar = 100 μm (F: 200×). *P < 0.05, **P < 0.01 and ***P < 0.001.

and si-ZBTB46-AS1 2#) and transfected them into SKOV3 and A2780 cell lines to suppress the expression of ZBTB46-AS1 in ovarian cancer cells. After 48 h of transfection, qRT-PCR was performed to measure the RNA expression levels of ZBTB46-AS1 in the two cell lines. We confirmed that si-ZBTB46-AS1 1# and si-ZBTB46-AS1 2# cells demonstrated a significant reduction in ZBTB46-AS1 expression compared to the control group (**Figure 2A**), indicating a successful downregulation of ZBTB46-AS1. Subsequently, the biological phenotypes of the cells were investigated. CCK-8 and Cell colony formation experiments revealed that ZBTB46-AS1 knockdown significantly inhibited the proliferation of SKOV3 and A2780 cells (**Figure 2B-E**). Similarly, the Transwell assay demonstrated that the migration ability of OC cells after ZBTB46-AS1 knockdown was significantly reduced (**Figure 2F** and **2G**). These findings implied that ZBTB46-AS1 promotes OC cell proliferation and migration in vitro.

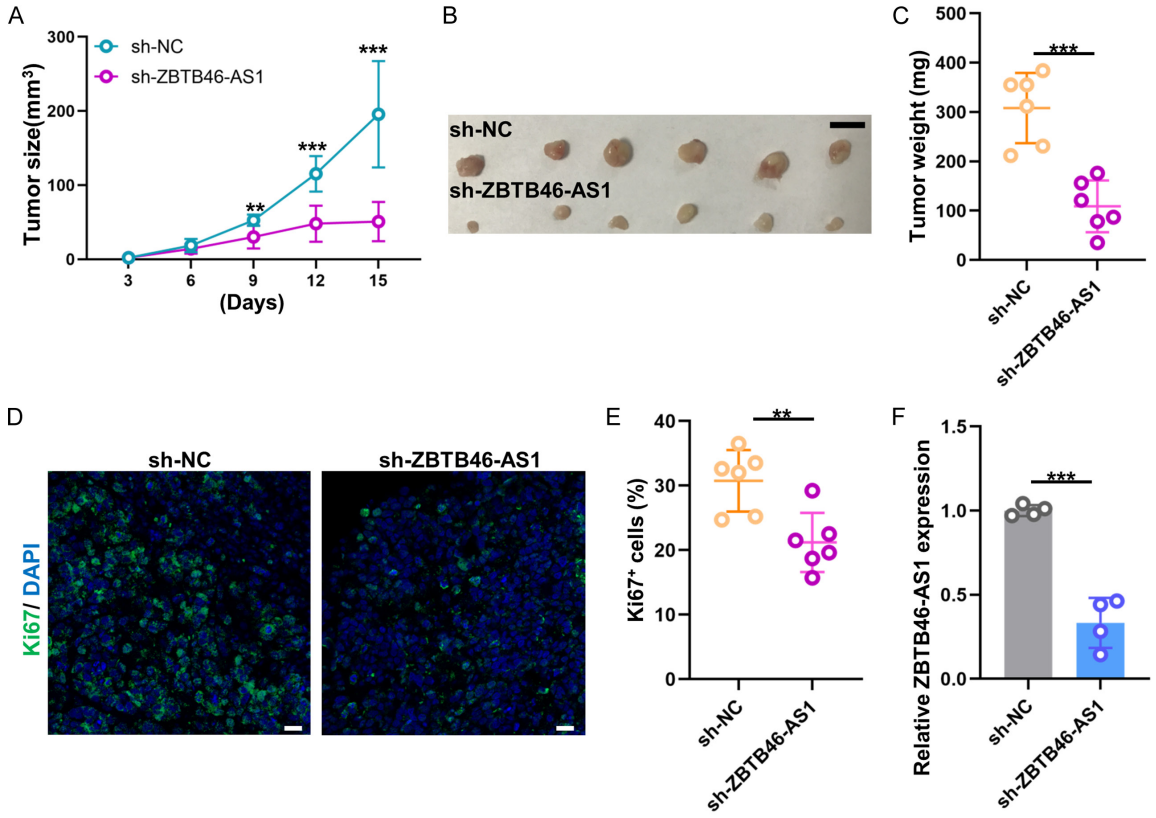


**Figure 3.** Effects of ZBTB46-AS1 knockdown on OC cell viability in vivo. (A) SKOV3 cells stably expressing sh-ZBTB46-AS1 or an empty vector (sh-NC) were injected into the underarms of nude mice, and tumor volumes were calculated every 3 days after injection (n = 6). (B, C) Tumors were removed from nude mice, photographed, and their weights were recorded. Scale bar = 1 cm (B: 5×). (D, E) Immunostaining for the Ki67 proliferation index in tumor sections (n = 3). Scale bar = 20 μm (D: 200×). (F) Relative ZBTB46-AS1 expression in tumors was detected by RT-qPCR. *P < 0.05, **P < 0.01 and ***P < 0.001.

*ZBTB46-AS1 promotes OC growth and metastasis in vivo*

To explore the in vivo effects of ZBTB46-AS1 on OC cells, we subcutaneously injected nude mice with stably transfected sh-ZBTB46-AS1 or control ovarian cancer cells to create a subcutaneous tumor model. These findings revealed that the downregulation of ZBTB46-AS1 substantially inhibited tumor development. The mice were euthanized after two weeks, and tumor tissues were collected. Compared to the control group, downregulation of ZBTB46-AS1 expression significantly reduced tumor size and weight (**Figure 3A-C**). Furthermore, immunohistochemistry (IHC) staining demonstrated a significant reduction in Ki67 expression in tumors from the ZBTB46-AS1 knockdown group (**Figure 3D** and **3E**). RT-qPCR detection confirmed that ZBTB46-AS1 was effectively knocked down in the tumor tissues of the sh-ZBTB46-AS1 group (**Figure 3F**).

Distant metastasis is a critical malignant biological characteristic of OC and is a primary cause of patient mortality. Therefore, we established an OC lung metastasis model, as shown in **Figure 4A** and **4B**. The number of lung metastases was significantly reduced in nude mice with ZBTB46-AS1 knockdown compared to that in the control group, implying that ZBTB46-AS1 promotes OC lung metastasis in vivo. Similar results were obtained using HE staining (**Figure 4C**).

EMT occurs when epithelial cells transform into mesenchymal cells and is implicated in the malignant progression of tumors [21]. During EMT, epithelial cells acquire mesenchymal properties and exhibit enhanced cellular motility and migration. This is manifested by the loss of epithelial markers, such as E-cadherin, and the upregulation of mesenchymal markers, such as N-cadherin and vimentin [22]. Using immunofluorescence staining, we observed that the

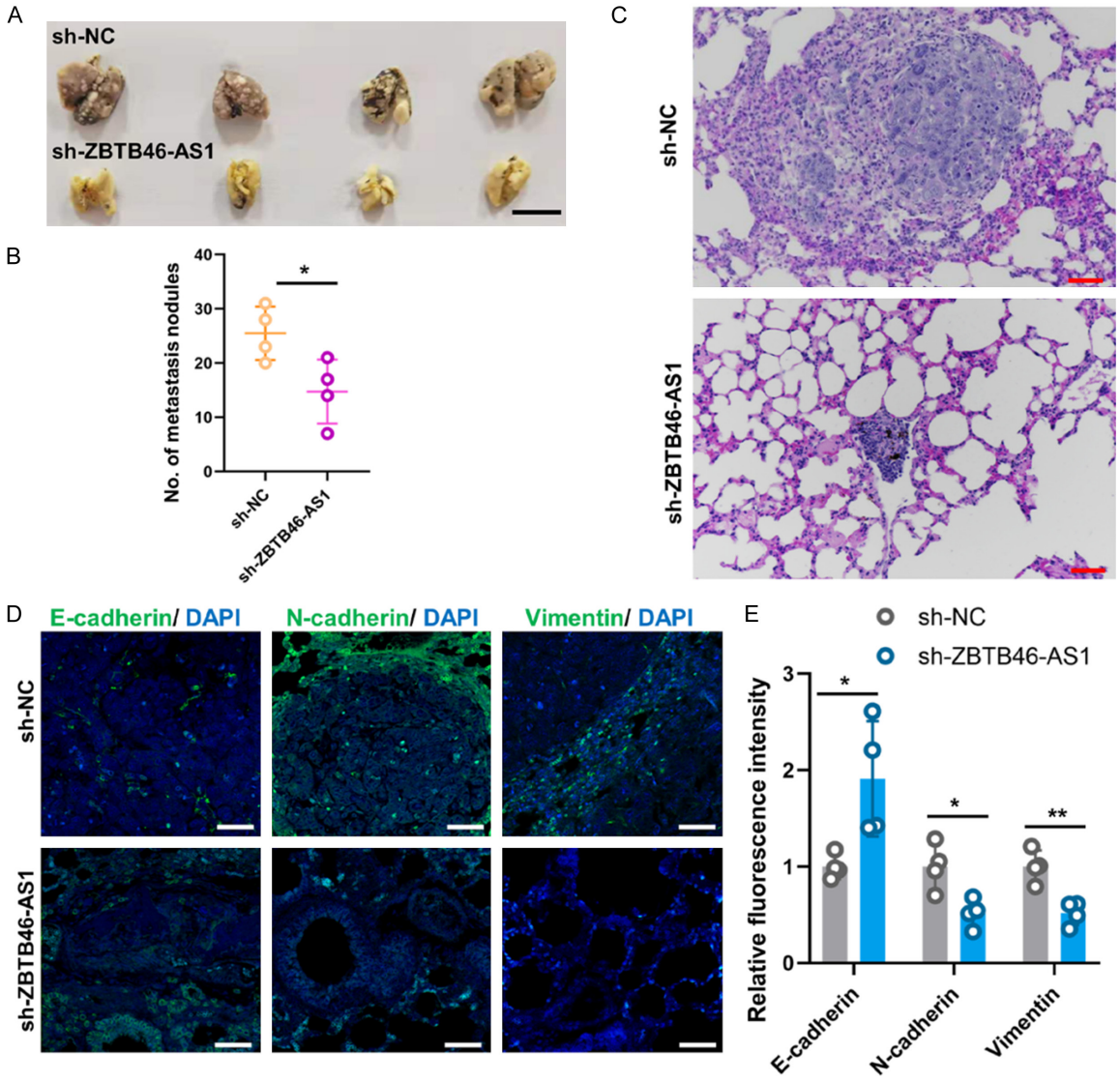


**Figure 4.** Effects of ZBTB46-AS1 knockdown on OC metastasis in vivo. (A) SKOV3 cells were transfected with sh-ZBTB46-AS1 or an empty vector and injected into the tail vein of nude mice (n = 4). After 2 months, the lung tissues were removed and photographed. Scale bar = 1 cm (A: 5×). (B) Number of lung nodules were counted. (C) H&E staining of paraffin sections from mouse lung tissues. Scale bar = 100 μm (C: 100×). (D) Multiplex immunofluorescence staining of EMT in OC progression. Scale bar = 50 μm (D: 200×). (E) Quantification of (D). *P < 0.05, **P < 0.01 and ***P < 0.001.

downregulation of ZBTB46-AS1 suppressed the expression of N-cadherin and vimentin, but increased the expression of E-cadherin (**Figure 4D** and **4E**). These findings suggest that ZBTB46-AS1 promotes ovarian cancer cell proliferation and migration, and induces EMT.

*ZBTB46-AS1 acts on the target protein TAF6*

To further characterize the proteins that interact with ZBTB46-AS1 in OC, we performed biotin-labeled RNA pull-down assays on SKOV3 cells to isolate the protein complexes associated with ZBTB46-AS1, followed by proteomic analysis of the pull-down products (**Figure 5A**). We identified two overlapping proteins, TAF6 and DNAJC9, in three independent RNA pull-down experiments using label-free quantitation (LFQ) analysis with a Venn diagram, as shown in the graph (**Figure 5B**). The transcription initiation factor TFIID Subunit 6 (TAF6) exhibited the highest expression levels. Based on the literature review, TAF6 was selected as the main protein of interest for further investigation

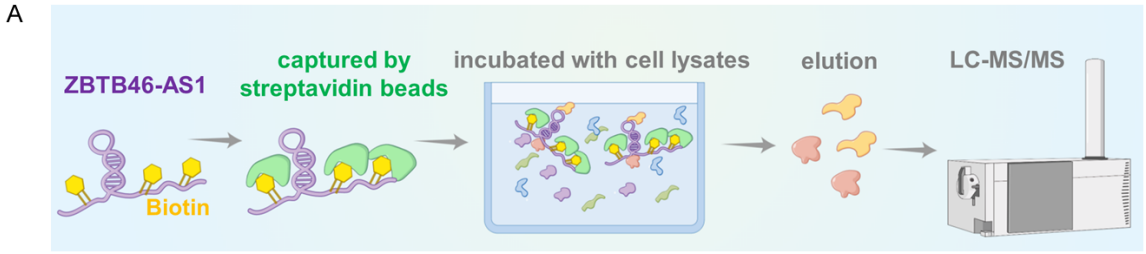


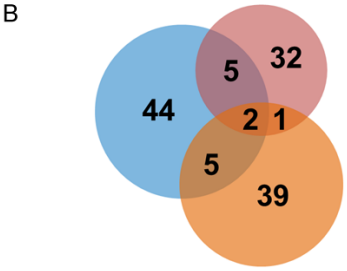


C

| Gene names | Replicates | iBAQ | |
|---|---|---|---|
| | | ZBTB46-AS1 | Control |
| TAF6 | 1 | 8539.2 | 0 |
| | 2 | 13245 | 0 |
| | 3 | 6810.6 | 0 |
| DNAJC9 | 1 | 3836.8 | 0 |
| | 2 | 4545.9 | 0 |
| | 3 | 4581.9 | 0 |

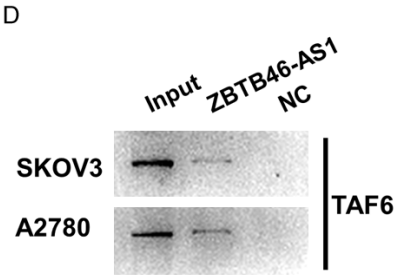


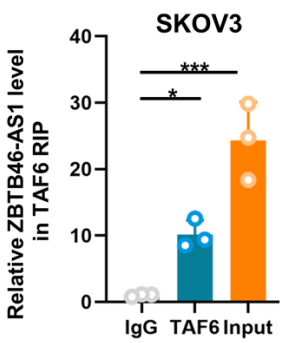


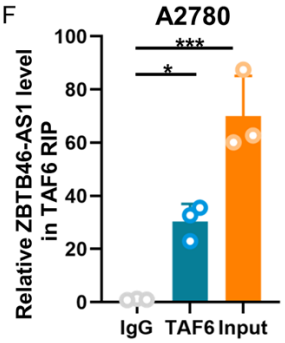


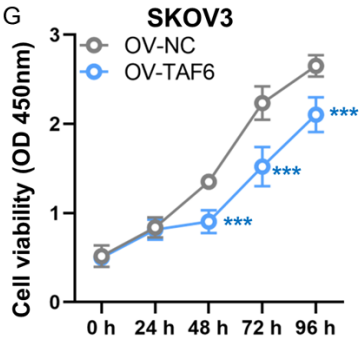


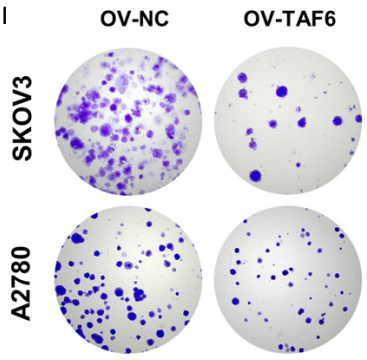


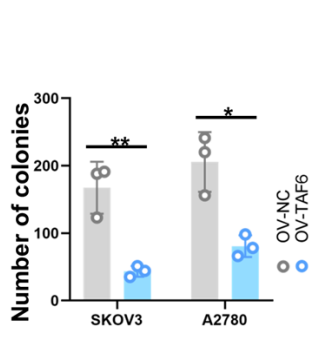


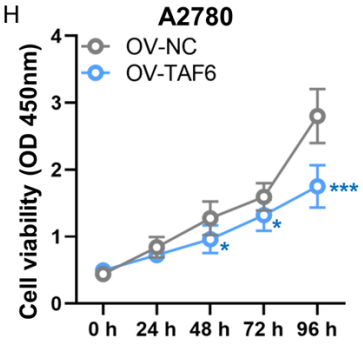


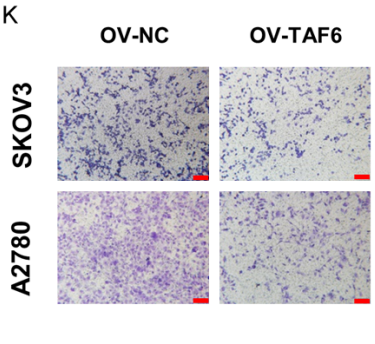


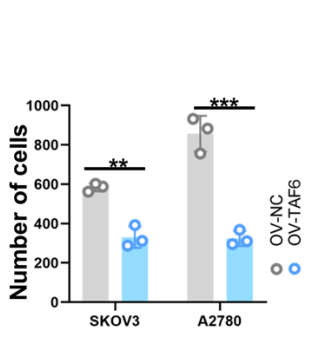


**Figure 5.** ZBTB46-AS1 interacts with TAF6. A. Flow chart of RNA pull-down assays. B. Venn analysis of the RNA-protein interactome in ovarian cancer cells. C. Two overlapping proteins are shown. D. Validation of the TAF6 interaction in RNA-protein complexes. E, F. RNA immunoprecipitation (RIP) assay for the interaction between ZBTB46-AS1 and TAF6 in OC cell lysates (n = 3 for each group). G-L. TAF6 suppressed the proliferation and migration capacity of OC cells in vitro. Assessment of proliferative and migratory phenotypes in OC cell lines following TAF6 overexpression (n = 3. Scale bar = 100 μm. (K: 200×). *P < 0.05, **P < 0.01 and ***P < 0.001).

(**Figure 5C**). SKOV3 and A2780 cell extracts were used for western blot analysis and RNA immunoprecipitation (RIP) assays to further validate the interaction between ZBTB46-AS1 and TAF6 (**Figure 5D-F**).

*TAF6 overexpression suppresses the proliferation and migration ability of OC cells in vitro*

To explore the role of TAF6 in OC, we overexpressed it in SKOV3 and A2780 cells. CCK-8 and cell clonal formation experiments revealed that TAF6 overexpression drastically reduced OC cell proliferation, viability, and colony formation (**Figure 5G-J**). Similarly, Transwell assays revealed that the number of migrated OC cells in the TAF6 overexpression group was lower than that in the control group (**Figure 5H-L**). These findings suggested that TAF6 inhibits OC cell proliferation and migration in vitro.

*ZBTB46-AS1 attenuates p53 activity through TAF6 protein*

Thut et al. [23] discovered that TAF6 directly interacts with the activation domain of p53, making it a critical target for transmitting the activation signal between p53 and the initiation complex. Therefore, we conducted dual-luciferase reporter assays to assess the regulatory effects of ZBTB46-AS1 and TAF6 on p53 activity in OC cells. We found that ZBTB46-AS1 knockdown or TAF6 overexpression in SKOV3 and A2780 cells significantly increased p53 activity compared with that in the control group. Conversely, ZBTB46-AS1 overexpression or TAF6 knockdown dramatically inhibited p53 activity (**Figure 6A** and **6B**). To confirm the mechanistic relevance, we detected p21 (CDKN1A), a canonical p53 target. RT-qPCR results (Figure S1) showed that p21 expression was significantly upregulated by ZBTB46-AS1 knockdown or TAF6 overexpression, and suppressed by ZBTB46-AS1 overexpression or TAF6 knockdown, consistent with p53 activity changes. To elucidate the interaction between these three factors, we first examined variations in TAF6 expression in response to ZBTB46-AS1 knockdown or overexpression. Interestingly, whether ZBTB46-AS1 was knocked down or overexpressed in SKOV3 and A2780 cells, western blotting indicated that TAF6 expression levels remained unchanged (**Figure 6C-F**), demonstrating that ZBTB46-AS1 did not affect the stability of the TAF6 protein. Co-immunoprecipitation (Co-IP) experiments were performed on SKOV3 and A2780 cells, and the results showed that knockdown or overexpression of ZBTB46-AS1 significantly influenced the interaction between TAF6 and p53. The interaction between TAF6 and p53 was enhanced following ZBTB46-AS1 knockdown, whereas ZBTB46-AS1 overexpression weakened the interaction between TAF6 and p53 (**Figure 6G** and **6H**). Based on these findings, we propose that ZBTB46-AS1 modulates the transcriptional activity of p53 by influencing the assembly of TAF6-p53 complexes by binding to the TAF6 protein, thus controlling p53 target genes such as p21.

*Simultaneous knockdown of ZBTB46-AS1 and p53 reversed the regulatory effect of ZBTB46-AS1 on OC cell behavior*

Functional rescue experiments were performed to elucidate the regulatory mechanism of ZBTB46-AS1 in OC. Co-transfection with si-ZBTB46-AS1 and si-p53 effectively mitigated the cellular phenotype inhibition induced by ZBTB46-AS1 knockdown alone, as demonstrated by CCK8, Cell clonal formation experiments, and Transwell assays (**Figure 7A-F**). This implies that ZBTB46-AS1 exerts its effects through the p53 pathway. In summary, our findings support the following observations: ZBTB46-AS1 inhibits the interaction between TAF6 and p53 by binding to the TAF6 protein, decreasing the activity of the transcription factor p53, and promoting the proliferation and migration of OC cells (**Figure 7G**).

## Discussion

Most patients with OC are often diagnosed at an advanced stage with tumor metastases, missing out on surgical treatment opportunities, which leads to a poor prognosis. However, considering that only a few therapeutic targets for OC have been identified, there is room for further research on alternative therapies. The biological functions of lncRNAs are complex and diverse, and lncRNAs are widely recognized as essential molecules that mediate gene transcription and regulation [24]. A substantial body of research has highlighted the significant role of lncRNAs in the pathogenesis of various human cancers including OC. Therefore, inves-

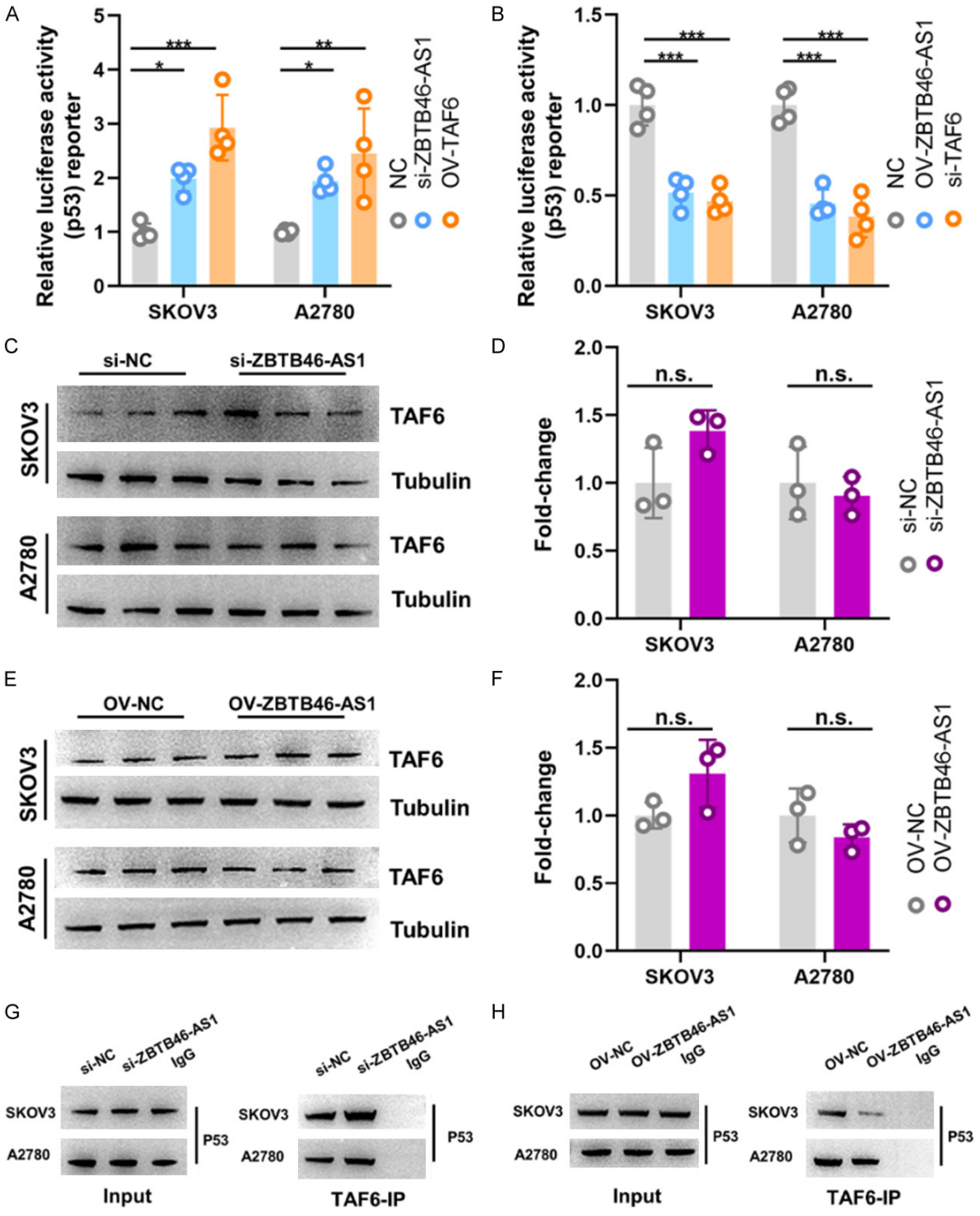


**Figure 6.** ZBTB46-AS1 regulates p53 activity by interacting with TAF6. (A, B) Dual-luciferase reporter assay was performed to measure p53 transcriptional activity. Distinct transfection groups were established in A2780 and SKOV3 cells by co-transfecting the luciferase reporter plasmid, pGL3-p53-TA-luc, with siRNA plasmids targeting ZBTB46-AS1 (si-ZBTB46-AS1), TAF6 (si-TAF6), or overexpression plasmids for ZBTB46-AS1 (OV-ZBTB46-AS1). Following a 48-hour incubation period, luciferase activity was evaluated using the Dual-Luciferase Reporter Assay Kit. (n = 3). (C) Western blotting analysis of TAF6 expression after ZBTB46-AS1 downregulation in SKOV3 and A2780 cells. (D) Quantification of (C). (E) Western blotting analysis of TAF6 expression after ZBTB46-AS1 overexpression in SKOV3 and A2780 cells. (F) Quantification of (E). (G, H) CO-IP assays were used to test the binding between TAF6 and p53. Three independent experiments were performed. *P < 0.05, **P < 0.01 and ***P < 0.001; ns: not significant (P > 0.05).

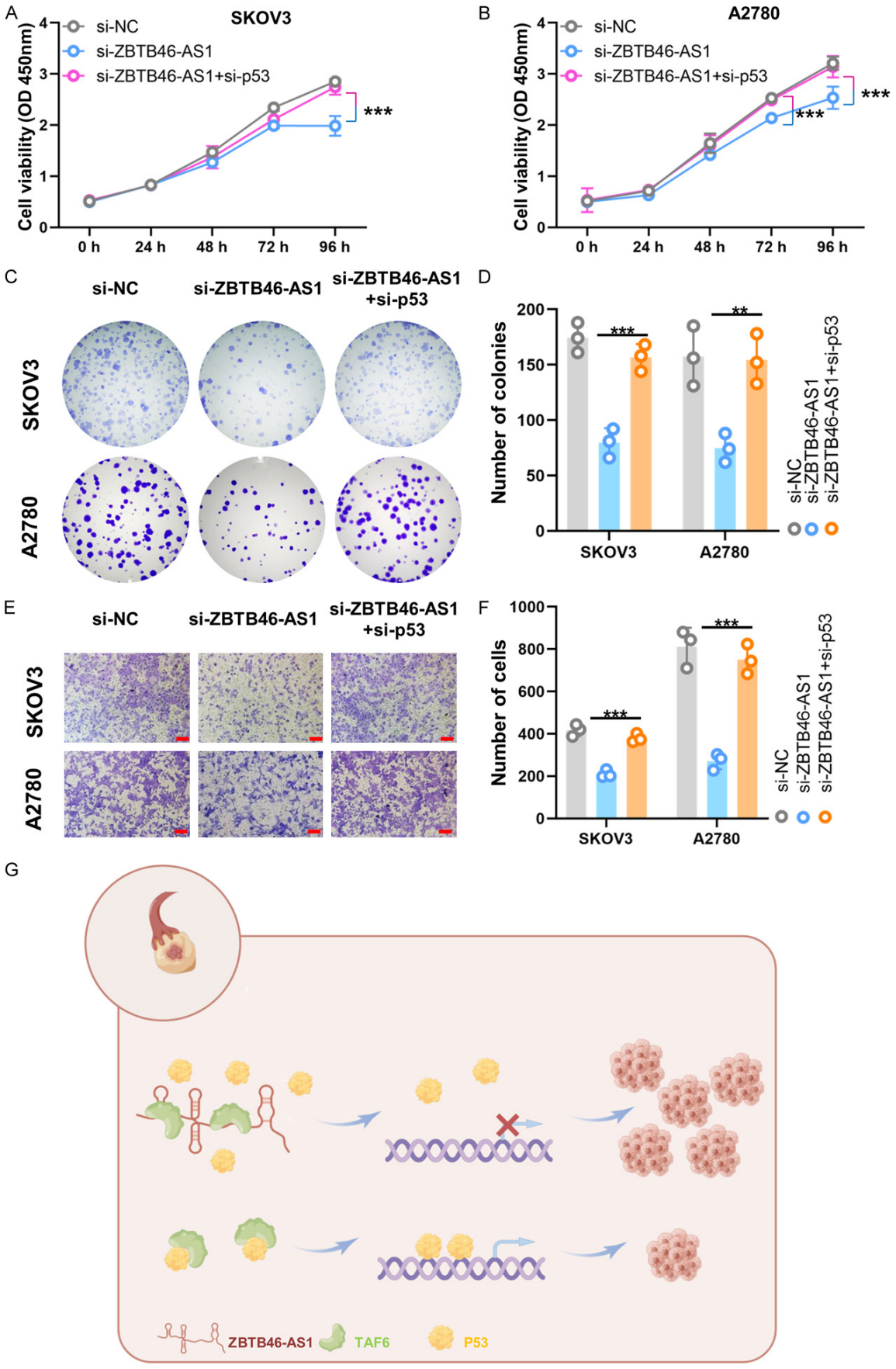
A
SKOV3
si-NC
si-ZBTB46-AS1
si-ZBTB46-AS1+si-p53
Cell viability (OD 450nm)
0 h
24 h
48 h
72 h
96 h
***
B
A2780
si-NC
si-ZBTB46-AS1
si-ZBTB46-AS1+si-p53
Cell viability (OD 450nm)
0 h
24 h
48 h
72 h
96 h
***
***
C
si-NC
si-ZBTB46-AS1
si-ZBTB46-AS1 +si-p53
SKOV3
A2780
D
Number of colonies
***
**
SKOV3
A2780
si-NC
si-ZBTB46-AS1
si-ZBTB46-AS1+si-p53
E
si-NC
si-ZBTB46-AS1
si-ZBTB46-AS1 +si-p53
SKOV3
A2780
F
Number of cells
***
***
SKOV3
A2780
si-NC
si-ZBTB46-AS1
si-ZBTB46-AS1+si-p53
G
ZBTB46-AS1
TAF6
P53

**Figure 7.** Simultaneous knockdown of ZBTB46-AS1 and p53 reversed the regulatory effect of ZBTB46-AS1 on OC cell behavior. (A, B) SKOV3 and A2780 cells were co-transfected with si-NC, si-ZBTB46-AS1, or si-ZBTB46-AS1+si-p53, and the proliferative ability of OC cells was detected using CCK8 assays at a specified time point. (C) Growth of SKOV3 and A2780 cells was evaluated using a colony formation assay. (D) Quantification of (C). (E) Cell migration of SKOV3 and A2780 cells was detected using Transwell assays. (F) Quantification of E. Scale bar = 100 μm (E: 200×). *P < 0.05, **P < 0.01 and ***P < 0.001. (G) Schematic representation of the ZBTB46-AS1-mediated oncogenic regulation of OC.

tigating the biological mechanisms and regulatory effects of lncRNAs in OC can potentially lead to innovative therapeutic approaches for OC treatment [25-27].

In our study, ZBTB46-AS1 was markedly upregulated in OC cell lines (A2780 and SKOV3) and in clinical specimens (n = 22). High expression levels independently predicted a poor prognosis. To investigate the functional role of ZBTB46-AS1 in OC, we used specific siRNAs to construct OC cell models with low ZBTB46-AS1 expression (si-ZBTB46-AS1#1 and si-ZBTB46-AS1#2). We then assessed the impact of ZBTB46-AS1 knockdown on OC cell proliferation and metastasis in vitro using a suite of assays, including CCK-8, clonal cell formation, and Transwell migration assays. A nude mouse xenograft model was used to evaluate the in vivo effects of the ZBTB46-AS1 knockdown on OC cell growth and metastasis. Our data revealed that ZBTB46-AS1 actively promoted OC cell growth and metastasis both in vitro and in vivo, suggesting its role as an oncogenic driver in OC tumorigenesis. Importantly, ZBTB46-AS1 has not been extensively studied to date; thus, our findings contribute a new perspective to the understanding of this area.

We further explored the mechanistic underpinnings of ZBTB46-AS1 in OC by focusing on its interaction with TAF6. This interaction was initially probed using Biotin-labeled RNA pull-down assays, with subsequent validation by western blotting and RNA immunoprecipitation (RIP) assays. TAF6, a core subunit of the RNA polymerase II transcription factor (TFIID), interacts with multiple proteins, including TAF9, TAF12, and TAF1, to form intricate preloaded and polymerase complexes that dynamically regulate gene expression during transcription initiation. Multiple subtypes of TAF6 splice variants have been identified, with the most researched being the widely expressed primary TAF6a and inducible TAF6δ subtypes [28, 29]. TAF6, with its high pro-apoptotic activity, has been established as a critical factor for the survival of various organisms, including humans. Moreover, TAF6 has been implicated in the proliferation and differentiation of stem cells and tumor cells, positioning it as a potential therapeutic target for disorders stemming from apoptotic dysregulation, such as cancer [30-33]. Notably, experimental evidence from TAF6 gene-deletion mouse models points to the development of cellular transformation characteristics and tumorigenesis, underscoring the essential role of TAF6 in tumor suppression [34, 35].

As a pivotal transcription factor, p53 orchestrates gene expression, which is pivotal for cell cycle arrest and apoptosis induction, thereby playing an essential role in safeguarding genomic integrity and tumor suppression [36, 37]. p53 primarily functions by activating its downstream target genes. In response to DNA damage, p53 specifically binds to its target genes within response elements (RE) in a dimeric form, recruiting a variety of transcriptional regulatory factors. This action leads to the activation or repression of target gene transcription, thereby modulating gene expression. Such intricate regulation is crucial for the p53-dependent apoptotic response to DNA damage [38, 39]. Extensive research has confirmed that the genesis of most tumors is linked to TP53 mutations or factors that hinder p53 transcriptional activation, leading to dysregulation of the p53 pathway [36, 40]. To date, more than 125 protein-coding genes and non-coding RNAs have been identified as direct transcriptional targets of p53, facilitating transcriptional activation upon p53 induction [41].

P53-mediated transcriptional activation is initiated by the binding of p53 to specific recognition sites within the promoter regions of target genes. In eukaryotes, transcription initiation is commonly triggered by the formation of the pre-initiation complex (PIC), which includes RNA polymerase II and six basal transcription factors: TFIIA, TFIIB, TFIID, TFIIE, TFIIF, and TFIIH. The TFIID complex, a multiprotein assem-

bly, is a general transcription factor that interacts with gene promoters and directs the transcription of approximately 90% of protein-coding genes. It exerts a pivotal regulatory influence on the transcriptional machinery of protein-coding genes in eukaryotes [42, 43]. TFIID recognizes and binds to multiple core promoter elements, and p53 has been shown to recruit TFIID to promoter regions, enhancing the binding of the transcription factor TFIID to gene promoters, thereby promoting gene expression [44, 45]. Moreover, several studies have indicated that in the absence of p53, assembly of the pre-initiation complex (PIC) is impeded, and TFIID recognition of the core promoter is diminished, constraining transcription initiation [46, 47]. Consequently, the interaction between p53 and TFIID components (e.g., TAFs) is essential for transcription initiation, enabling the recruitment of RNA polymerase II to target gene promoters. TAF6 can function as a coactivator of p53, especially in the context of p53-mediated gene regulation. Studies have demonstrated that TAF6 and p53 exhibit functional interactions during assembly of the transcription initiation complex [48]. The TAF6-p53 complex enhances p53 DNA-binding and transcriptional activity, enabling the precise regulation of genes involved in DNA repair and tumor suppression pathways [49].

In a subsequent series of experiments, we conducted immunoprecipitation assays to determine physical interactions between TAF6 and p53. These results unequivocally demonstrated that p53 is capable of co-precipitating with TAF6, indicating a direct interaction between these two critical proteins. Moreover, our findings indicate that the overexpression of ZBTB46-AS1 significantly diminishes the interaction between TAF6 and p53. Conversely, the knockdown of ZBTB46-AS1 led to enhanced interactions, implying that the levels of ZBTB46-AS1 may modulate the formation of the TAF6-p53 complex. This modulation is anticipated to exert downstream effects on the p53 transcriptional activation of its target genes, thereby influencing cellular responses.

In further experiments, we constructed a firefly luciferase reporter gene vector containing a p53 response element and meticulously designed multiple transfection groups to investigate the effects of ZBTB46-AS1 and TAF6 on p53 activity. The reduction in luciferase activity indicated that both overexpression of lncRNA ZBTB46-AS1 and knockdown of TAF6 repressed p53 expression. Simultaneously, Western blot analysis revealed that TAF6 expression levels remained unaltered irrespective of whether lncRNA ZBTB46-AS1 was knocked down or overexpressed. This observation suggests that lncRNA ZBTB46-AS1 does not affect the stability of the TAF6 protein; instead, it appears to engage in a direct interaction with TAF6, potentially influencing the transcriptional landscape governed by the TAF6-p53 axis.

Based on our experimental observations, we speculate that in OC, elevated levels of ZBTB46-AS1 modulate the formation of the TAF6-p53 complex by directly interacting with TAF6. This interaction has been proposed to inhibit p53's transcriptional activation capacity on its target genes. This speculation was consistent with the results of our subsequent in vitro experiments, in which we found that TAF6 overexpression diminished OC cell proliferation and migration capabilities, consistent with the effects observed after siRNA-mediated knockdown of ZBTB46-AS1. Ultimately, rescue experiments confirmed that the concurrent knockdown of ZBTB46-AS1 and p53 rescued the migration and proliferation of OC cells, which were suppressed by siRNA-mediated knockdown of ZBTB46-AS1.

In conclusion, our study is the first to reveal the upregulation of ZBTB46-AS1 in OC and its critical role in tumor progression. Moreover, we not only confirmed the promoting effects of ZBTB46-AS1 on OC cell proliferation and migration but also offered new theoretical support and experimental evidence for understanding the regulatory mechanisms of ZBTB46-AS1 on p53 activity, thereby presenting potential therapeutic targets for the molecular treatment of OC.

## Acknowledgements

This work was supported by Suzhou Science and Technology Plan Project (No. SKY2021056) and Suzhou "Science and Education for Health" Youth Science and Technology Program (No. KJXW2023032).

## Disclosure of conflict of interest

None.

**Address correspondence to:** Hong Xu, Department of Oncology, The First Affiliated Hospital of Soochow University, Suzhou 215006, Jiangsu, China. Tel: +86-13301549066; E-mail: 13301549066@163.com; Fen Guo, Department of Oncology, The Affiliated Suzhou Hospital of Nanjing Medical University, Suzhou Municipal Hospital, Gusu School, Nanjing Medical University, Suzhou 215008, Jiangsu, China. Tel: +86-17798695787; E-mail: guof123@126.com

## References

[1] Siegel RL, Miller KD, Wagle NS and Jemal A. Cancer statistics, 2023. CA Cancer J Clin 2023; 73: 17-48.

[2] Berek JS, Renz M, Kehoe S, Kumar L and Friedlander M. Cancer of the ovary, fallopian tube, and peritoneum: 2021 update. Int J Gynaecol Obstet 2021; 155 Suppl 1: 61-85.

[3] Esteller M. Non-coding RNAs in human disease. Nat Rev Genet 2011; 12: 861-874.

[4] Ponting CP, Oliver PL and Reik W. Evolution and functions of long noncoding RNAs. Cell 2009; 136: 629-641.

[5] Sun Q, Hao Q and Prasanth KV. Nuclear long noncoding RNAs: key regulators of gene expression. Trends Genet 2018; 34: 142-157.

[6] Chen LL. Linking long Noncoding RNA localization and function. Trends Biochem Sci 2016; 41: 761-772.

[7] Wei JW, Huang K, Yang C and Kang CS. Noncoding RNAs as regulators in epigenetics (Review). Oncol Rep 2017; 37: 3-9.

[8] Akhade VS, Pal D and Kanduri C. Long noncoding RNA: genome organization and mechanism of action. Adv Exp Med Biol 2017; 1008: 47-74.

[9] Zamaraev AV, Volik PI, Sukhikh GT, Kopeina GS and Zhivotovsky B. Long non-coding RNAs: a view to kill ovarian cancer. Biochim Biophys Acta Rev Cancer 2021; 1876: 188584.

[10] Lee SU and Maeda T. POK/ZBTB proteins: an emerging family of proteins that regulate lymphoid development and function. Immunol Rev 2012; 247: 107-119.

[11] Satpathy AT, Kc W, Albring JC, Edelson BT, Kretzer NM, Bhattacharya D, Murphy TL and Murphy KM. Zbtb46 expression distinguishes classical dendritic cells and their committed progenitors from other immune lineages. J Exp Med 2012; 209: 1135-1152.

[12] Zhou W, Zhou L and Zhou J; JRI Live Cell Bank; Chu C, Zhang C, Sockolow RE, Eberl G and Sonnenberg GF. ZBTB46 defines and regulates ILC3s that protect the intestine. Nature 2022; 609: 159-165.

[13] Zhao D, Shen C, Gao T, Li H, Guo Y, Li F, Liu C, Liu Y, Chen X, Zhang X, Wu Y, Yu Y, Lin M, Yuan Y, Chen X, Huang X, Yang S, Yu J, Zhang J and Zheng B. Myotubularin related protein 7 is essential for the spermatogonial stem cell homeostasis via PI3K/AKT signaling. Cell Cycle 2019; 18: 2800-2813.

[14] Gao T, Lin M, Shao B, Zhou Q, Wang Y, Chen X, Zhao D, Dai X, Shen C, Cheng H, Yang S, Li H, Zheng B, Zhong X, Yu J, Chen L and Huang X. BMI1 promotes steroidogenesis through maintaining redox homeostasis in mouse MLTC-1 and primary Leydig cells. Cell Cycle 2020; 19: 1884-1898.

[15] Shen C, Zhang K, Yu J, Guo Y, Gao T, Liu Y, Zhang X, Chen X, Yu Y, Cheng H, Zheng A, Li H, Huang X, Ding X and Zheng B. Stromal interaction molecule 1 is required for neonatal testicular development in mice. Biochem Biophys Res Commun 2018; 504: 909-915.

[16] Zhou J, Li J, Qian C, Qiu F, Shen Q, Tong R, Yang Q, Xu J, Zheng B, Lv J and Hou J. LINC00624/TEX10/NF-kappaB axis promotes proliferation and migration of human prostate cancer cells. Biochem Biophys Res Commun 2022; 601: 1-8.

[17] Jiang B, Wang K, Hu H, Gao W, Shen C, Chen X, Huang X, Yu J, Wu Y and Zheng B. CRL2LRRC41-mediated DDX5 ubiquitination enhances interaction with ELAVL1 preventing NOG mRNA degradation and sustaining proliferation and migration of human spermatogonial stem cell-like cell line. BMC Biol 2025; 23: 247.

[18] Lv J, Wu T, Xue J, Shen C, Gao W, Chen X, Guo Y, Liu M, Yu J, Huang X and Zheng B. ASB1 engages with ELOB to facilitate SQOR ubiquitination and H2S homeostasis during spermiogenesis. Redox Biol 2025; 79: 103484.

[19] Hu H, Xi X, Jiang B, Wang K, Wu T, Chen X, Guo Y, Zhou T, Huang X, Yu J, Gao T, Wu Y and Zheng B. RNF187 facilitates proliferation and migration of human spermatogonial stem cells through WDR77 polyubiquitination. Cell Prolif 2025; 58: e70042.

[20] Shen C, Cao R, Zhou Q, Zhou T, Wu T, Gao W, Wang G, Feng G, Qiao L and Wang T. LINC00654 promotes ovarian cancer progression by facilitating nuclear export of HuR and stabilizing oncogenic mRNAs. Oncogene 2025; 44: 3422-3436.

[21] De Craene B and Berx G. Regulatory networks defining EMT during cancer initiation and progression. Nat Rev Cancer 2013; 13: 97-110.

[22] Singh M, Yelle N, Venugopal C and Singh SK. EMT: Mechanisms and therapeutic implications. Pharmacol Ther 2018; 182: 80-94.

[23] Thut CJ, Chen JL, Klemm R and Tjian R. p53 transcriptional activation mediated by coactivators TAFII40 and TAFII60. Science 1995; 267: 100-104.

[24] Yao RW, Wang Y and Chen LL. Cellular functions of long noncoding RNAs. Nat Cell Biol 2019; 21: 542-551.
[25] Zhu D, Shi C, Jiang Y, Zhu K, Wang X and Feng W. Cisatracurium inhibits the growth and induces apoptosis of ovarian cancer cells by promoting lincRNA-p21. Bioengineered 2021; 12: 1505-1516.
[26] Buttarelli M, De Donato M, Raspaglio G, Babini G, Ciucci A, Martinelli E, Baccaro P, Pasciuto T, Fagotti A, Scambia G and Gallo D. Clinical value of lncRNA MEG3 in high-grade serous ovarian cancer. Cancers (Basel) 2020; 12: 966.
[27] Liu J, Yan C and Xu S. LncRNA IL21-AS1 facilitates tumour progression by enhancing CD24-induced phagocytosis inhibition and tumorigenesis in ovarian cancer. Cell Death Dis 2024; 15: 313.
[28] Bieniossek C, Papai G, Schaffitzel C, Garzoni F, Chaillet M, Scheer E, Papadopoulos P, Tora L, Schultz P and Berger I. The architecture of human general transcription factor TFIID core complex. Nature 2013; 493: 699-702.
[29] Wilhelm E, Kornete M, Targat B, Vigneault-Edwards J, Frontini M, Tora L, Benecke A and Bell B. TAF6delta orchestrates an apoptotic transcriptome profile and interacts functionally with p53. BMC Mol Biol 2010; 11: 10.
[30] Lago C, Clerici E, Dreni L, Horlow C, Caporali E, Colombo L and Kater MM. The Arabidopsis TFIID factor AtTAF6 controls pollen tube growth. Dev Biol 2005; 285: 91-100.
[31] Aoyagi N and Wassarman DA. Developmental and transcriptional consequences of mutations in Drosophila TAF(II)60. Mol Cell Biol 2001; 21: 6808-6819.
[32] Amsterdam A, Nissen RM, Sun Z, Swindell EC, Farrington S and Hopkins N. Identification of 315 genes essential for early zebrafish development. Proc Natl Acad Sci U S A 2004; 101: 12792-12797.
[33] Poon D, Bai Y, Campbell AM, Bjorklund S, Kim YJ, Zhou S, Kornberg RD and Weil PA. Identification and characterization of a TFIID-like multiprotein complex from Saccharomyces cerevisiae. Proc Natl Acad Sci U S A 1995; 92: 8224-8228.
[34] Reed JC. Apoptosis-based therapies. Nat Rev Drug Discov 2002; 1: 111-121.
[35] Watson J. Oxidants, antioxidants and the current incurability of metastatic cancers. Open Biol 2013; 3: 120144.
[36] Vousden KH and Lane DP. p53 in health and disease. Nat Rev Mol Cell Biol 2007; 8: 275-283.
[37] Kruiswijk F, Labuschagne CF and Vousden KH. p53 in survival, death and metabolic health: a lifeguard with a licence to kill. Nat Rev Mol Cell Biol 2015; 16: 393-405.
[38] Shibue T, Takeda K, Oda E, Tanaka H, Murasawa H, Takaoka A, Morishita Y, Akira S, Taniguchi T and Tanaka N. Integral role of Noxa in p53-mediated apoptotic response. Genes Dev 2003; 17: 2233-2238.
[39] Bieging KT, Mello SS and Attardi LD. Unravelling mechanisms of p53-mediated tumour suppression. Nat Rev Cancer 2014; 14: 359-370.
[40] Oren M. Decision making by p53: life, death and cancer. Cell Death Differ 2003; 10: 431-442.
[41] Riley T, Sontag E, Chen P and Levine A. Transcriptional control of human p53-regulated genes. Nat Rev Mol Cell Biol 2008; 9: 402-412.
[42] Cler E, Papai G, Schultz P and Davidson I. Recent advances in understanding the structure and function of general transcription factor TFIID. Cell Mol Life Sci 2009; 66: 2123-2134.
[43] Burley SK and Roeder RG. Biochemistry and structural biology of transcription factor IID (TFIID). Annu Rev Biochem 1996; 65: 769-99.
[44] Singh SK, Qiao Z, Song L, Jani V, Rice W, Eng E, Coleman RA and Liu WL. Structural visualization of the p53/RNA polymerase II assembly. Genes Dev 2016; 30: 2527-2537.
[45] Coleman RA, Qiao Z, Singh SK, Peng CS, Cianfrocco M, Zhang Z, Piasecka A, Aldeborgh H, Basishvili G and Liu WL. p53 dynamically directs TFIID assembly on target gene promoters. Mol Cell Biol 2017; 37: e00085-17.
[46] Colgan J and Manley JL. TFIID can be rate limiting in vivo for TATA-containing, but not TATA-lacking, RNA polymerase II promoters. Genes Dev 1991; 6: 304-315.
[47] Chi T, Lieberman P, Ellwood K and Carey M. A general mechanism for transcriptional synergy by eukaryotic activators. Nature 1995; 377: 254-257.
[48] Jimenez GS, Nister M, Stommel JM, Beeche M, Barcarse EA, Zhang XQ, O'Gorman S and Wahl GM. A transactivation-deficient mouse model provides insights into Trp53 regulation and function. Nat Genet 2000; 26: 37-43.
[49] Johnson TM, Hammond EM, Giaccia A and Attardi LD. The p53QS transactivation-deficient mutant shows stress-specific apoptotic activity and induces embryonic lethality. Nat Genet 2005; 37: 145-152.

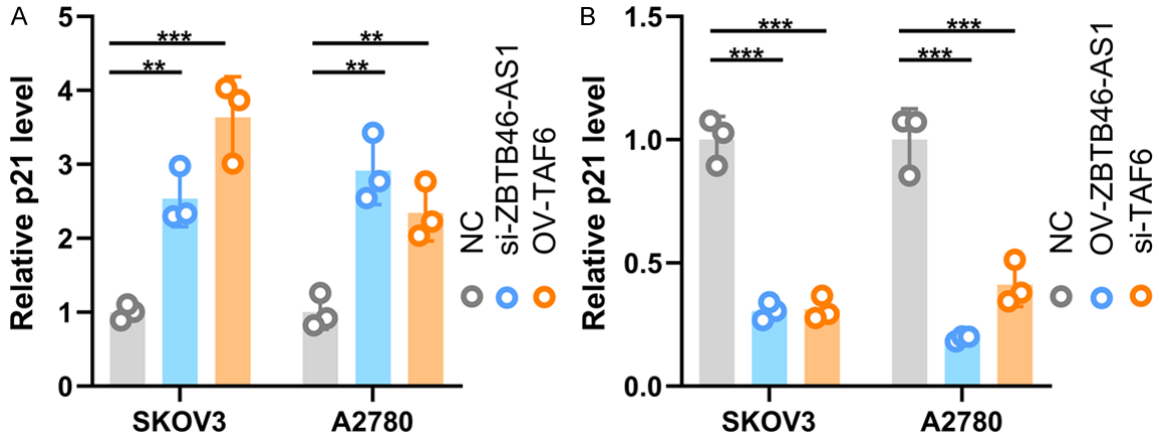


**Figure S1.** ZBTB46-AS1 regulates p53 activity by interacting with TAF6. A, B. RT-qPCR analysis of the expression level of a canonical p53 target, p21, in SKOV3 and A2780 cells transfected with the indicated siRNAs and plasmids. ZBTB46-AS1 knockdown or TAF6 overexpression in SKOV3 and A2780 cells significantly increased p21 expression compared with that in the control group. Conversely, ZBTB46-AS1 overexpression or TAF6 knockdown dramatically inhibited p21 expression. **P < 0.01 and ***P < 0.001.